Electronic Supplementary Information (ESI)

Versatile Thermally Activated Delayed Fluorescence Emitter for Both Highly Efficient Doped and Non-Doped Organic Light Emitting Devices

Wei-Lung Tsai, Ming-Hao, Huang, Wei-Kai Lee , Yi-Jiun Hsu, Kuan-Chung Pan, Yi-Hsiang Huang, Hao-Chun Ting, Monima Sarma, Yu-Yi Ho, Hung-Chieh Hu, Chung-Chia Chen, Meng-Ting Lee, Ken-Tsung Wong, and Chung-Chih Wu**

Experimental

Theoretical Methodology: Geometrical optimization in the ground state and orbital distributions for **DMAC-TAZ** were calculated with the Gaussian 09 program package at the B3LYP method with 6-311G(d) basis set, using the time-dependent density function theory (TD-DFT).

Thermal Properties: Differential scanning calorimetry (DSC) analyses were performed on a TA Instrument DSC-2920 Low-Temperature Difference Scanning Calorimeter at a heating rate of 20 ^{o}C min^{-1} from 50 to 380 ^{o}C under nitrogen. For the first run, the sample was heated to the temperature ca. 50 degree higher than its melting point to give an isotropic liquid sample. The sample was then quenched with liquid nitrogen before the second-run analysis. Thermogravimetric analysis (TGA) was undertaken with a TGA Q500 instrument. The thermal stability of the samples under a nitrogen atmosphere was determined by measuring their 5% weight loss while heating at a rate of 10 ^{o}C min^{-1} from 25 to 800 ^{o}C.

Photophysical Characterization: Synthesized compounds were subject to purification by temperature-gradient sublimation in high vacuum before use in subsequent studies. Thin films for photophysical characterization were prepared by thermal evaporation on quartz substrates at 1-2 Å/sec in a vacuum chamber with a base pressure of $<10^{-6}$ torr. Absorption spectra of the resulting thin films and dilute solutions were characterized by a UV-vis-NIR spectrophotometer (UV-1650 PC, Shimadzu). Photoluminescence (PL) spectra, photoluminescence quantum yields (PLQYs), and phosphorescence spectra were

characterized by a spectrofluorimeter (FluoroMax-P, Horiba Jobin Yvon Inc.). PLQYs of thin films or dilute solutions were determined using this spectrofluorimeter equipped with a calibrated integrating sphere. The selected monochromatic excitation light was used to excite samples placed in the calibrated integrating sphere. By comparing the spectral intensities of the monochromatic excitation light and the PL emission, the PL quantum yields were determined. Phosphorescence spectra of thin films or dilute solutions were conducted at 77 K (the liquid nitrogen temperature) by the spectrofluorometer equipped with a microsecond flash lamp as the pulsed excitation source. A 10-ms delay time was inserted between the pulsed excitation and the collection of the emission spectrum. Time-resolved PL (PL decay curves) was measured by monitoring the decay of the intensity at the PL peak wavelength using the time-correlated single-photon counting technique with a fluorescence lifetime system (FluoroCube, Horiba Jobin Yvon Inc.) and nanosecond pulsed light excitation from a UV light-emitting diode (300 nm). The samples were placed in a vacuum cryostat chamber with the temperature control. The PL spectra of the prompt and delayed components were collected using this same fluorescence lifetime system with a 200-ns delay time and a 10-μs delay time between the pulsed excitation and the collection of the emission spectrum.

Electrochemical Characterization: Cyclic voltammetry by a CHI 619B potentiostat was used to measure oxidation/reduction potentials. The oxidation potential was determined by cyclic voltammetry (CV) using 0.1M *n*-Bu_4NPF_6 ($TBAPF_6$) in CH_2Cl_2 as a supporting electrolyte and a scan rate of 100 mV s^{-1}. The reduction potential was recorded using 0.1M *n*-Bu_4NClO_4 (TBAP) in DMF as a supporting electrolyte and a scan rate of 100 mV s^{-1}. A standard 3-electrode cell comprising silver/silver chloride (Ag/AgCl), a platinum wire and a glassy carbon electrode as the reference, counter, and working electrodes, respectively, were used. All potentials were recorded versus Ag/AgCl (saturated) as a reference electrode. Oxidation of the ferrocene/ferrocenium (Fc/Fc^+) redox couple in CH_2Cl_2/$TBAPF_6$ occurs at E'_o = + 0.47

V and reduction of the ferrocene/ferrocenium (Fc/Fc^+) redox couple in DMF/TBAP occurs at E'_o = + 0.51 V vs. Ag/AgCl (saturated).

OLED Fabrication and Characterization: OLEDs were fabricated on the ITO-coated glass substrates with multiple organic layers sandwiched between the transparent bottom indium-tin-oxide (ITO) anode and the top metal cathode. The PEDOT:PSS layer was prepared by spin coating from the as-purchased aqueous dispersion of PEDOT:PSS (Clevios, Heraeus Co.), followed by annealing on a hot plate at 130 °C for 15 min. under ambient conditions. Other material layers were deposited by vacuum evaporation in a vacuum chamber with a base pressure of $<10^{-6}$ torr. All organic materials used in experiments (except for the TADF materials **DMAC-TRZ**, **PXZ-TRZ**) were purchased from Lumtec, Inc. The deposition system permits the fabrication of the complete device structure in a single vacuum pump-down without breaking vacuum. The deposition rate of organic layers was kept at ~0.1-0.2 nm/s. The doping was conducted by co-evaporation from two evaporation sources with different evaporation rates. The active area of the device is 1x1 mm^2, as defined by the shadow mask for cathode deposition. The current-voltage-brightness (I-V-L) characterization of the light-emitting devices was performed with a source-measurement unit (SMU) and a Si photodiode calibrated with a spectroradiometer (DMS 201, AUTRONIC-MELCHERS GmbH). EL spectra of devices were collected by a calibrated CCD spectrograph. The external quantum efficiencies of devices were determined by measuring the angular distribution of the emission spectra and intensities and were confirmed by collecting the total emission fluxes with a calibrated integrating-sphere measurement system.

Geometry data for **DMAC-TAZ** :

C	-6.18011	0.34388	2.49698	H	-7.96611	1.40265	0.69522
N	-3.46642	-0.00011	0.00002	H	-7.9664	-1.40207	-0.6954
C	-4.15193	-0.16295	-1.21733	H	-7.96663	-1.16003	1.05022
C	-5.55944	-0.17256	-1.255	H	-6.7126	-2.15131	0.29818
C	-6.42328	0.00011	-0.00004	H	-1.88231	2.12914	-0.21295
C	-3.42672	-0.31738	-2.41408	H	0.60907	2.12936	-0.20895
C	-4.07606	-0.4839	-3.62809	H	0.60915	-2.12943	0.20902
C	-5.4661	-0.49995	-3.67888	H	-1.88224	-2.12929	0.21303
C	-6.18004	-0.34383	-2.49704	C	2.25508	-0.00001	0.00002
C	-7.32105	1.25333	-0.1737	N	2.88033	-1.18064	0.07335
C	-5.4662	0.49985	3.67886	N	2.88029	1.18064	-0.07331
C	-4.07615	0.48361	3.62813	N	4.92848	0.00003	-0.00001
C	-3.42679	0.31705	2.41414	C	4.96073	2.41521	-0.14411
C	-4.15196	0.16278	1.21735	C	6.36217	2.42494	-0.15905
C	-5.55948	0.17257	1.25496	C	4.2697	3.63332	-0.19987
C	-7.32135	-1.25291	0.17356	C	7.05596	3.62751	-0.22854
C	-2.03144	-0.00008	0.00004	H	6.89275	1.4825	-0.11568
C	-1.32982	1.2006	-0.11956	C	4.96653	4.83421	-0.26854
C	0.05969	1.20139	-0.11729	H	3.18746	3.62259	-0.18741
C	0.77092	-0.00004	0.00004	C	6.36085	4.8351	-0.28327
C	0.05973	-1.20148	0.11737	H	8.14109	3.62394	-0.2399
C	-1.32978	-1.20074	0.11964	H	4.42185	5.77184	-0.31081
C	4.21944	1.13369	-0.06894	H	6.90376	5.77345	-0.33725
C	4.21948	-1.13364	0.06895	C	4.9608	-2.41514	0.14411
H	-5.98821	0.63038	4.62072	C	6.36224	-2.42483	0.159
H	-3.48863	0.60044	4.53326	C	4.26981	-3.63327	0.19991
H	-2.34541	0.3061	2.39156	C	7.05607	-3.62739	0.22847
H	-7.26372	0.35524	2.54295	H	6.89279	-1.48238	0.1156
H	-2.34535	-0.30657	-2.39145	C	4.96667	-4.83414	0.26857
H	-3.48851	-0.60084	-4.53319	H	3.18756	-3.62257	0.18749
H	-5.98809	-0.63044	-4.62076	C	6.36099	-4.83499	0.28324
H	-7.26365	-0.35504	-2.54306	H	8.14119	-3.62379	0.23979
H	-6.71208	2.15159	-0.29828	H	4.42201	-5.77178	0.31087
H	-7.96629	1.1606	-1.0504	H	6.90393	-5.77333	0.33721

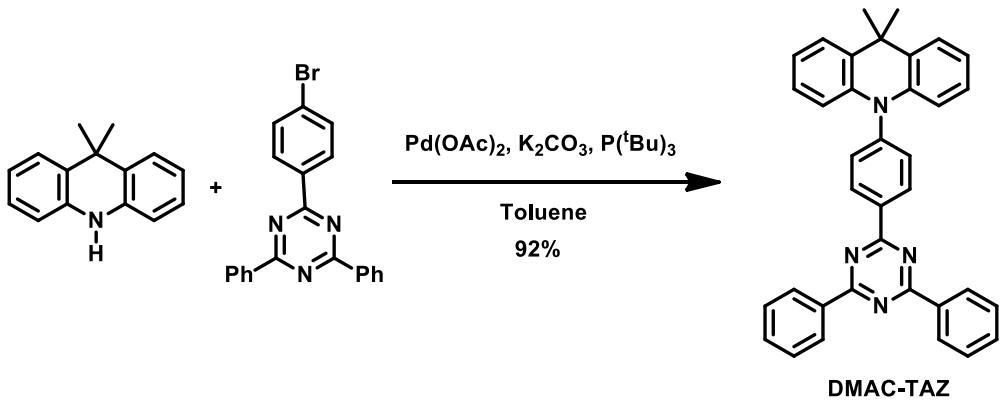

Scheme S1. Synthesis of **DMAC-TRZ**.

Synthesis of ***DMAC-TRZ***: 9,9-Dimethyl-9,10-dihydroacridine (1.0 g, 4.8 mmol), 2-(4-bromophenyl)-4,6-diphenyl-1,3,5-triazine (2.0 g, 5.28 mmol), potassium carbonate (2 g , 14.4 mmol), palladium(II) acetate (53 mg, 0.24 mmol) and toluene (50 mL) in a 100-mL two-necked flask, with stirring under argon atmosphere, was addd tri-tert-butylphosphine (0.05M 19 mL) with a syringe. The mixture was stirring and refluxed for two days. The cooled mixture was partitioned between EtOAc and water. The organic layer was separated, and the aqueous layer was extracted with chloroform. The combined organic layers were washed with brine, dried over $MgSO_4$ and concentrated by rotary evaporator. The residue was purified by column chromatography on silica gel (eluent: chloroform/hexane=1/4) to afford **DMAC-TRZ** (2.3 g, 4.42 mmol, 92%). mp 234 °C (DSC) ^{1}H NMR ($CDCl_3$, 400 MHz) δ (ppm) 9.05 (d, J = 8.0 Hz, 2H), 8.84 (d, J = 8.0 Hz, 4H), 7.59-7.68 (m, 8H), 7.53 (d, J = 8.0 Hz, 2H), 6.98-7.06 (m, 4H), 6.43 (d, J = 8.0 Hz, 2H), 1.73 (s, 6H). ^{13}C NMR ($CDCl_3$, 100 MHz) δ (ppm) 172.08, 171.31, 145.59, 140.87, 136.34, 136.32, 132.95, 131.87, 131.76, 130.51, 129.29, 128.97, 126.73, 125.63, 121.13, 114.47, 36.32, 31.58. HRMS (ESI, m/z) calcd for $C_{36}H_{28}N_4$, 516.2314; found 513.2378. Elemental analyses calcd. for $C_{36}H_{28}N_4$: C 83.69, H 5.46, N 10.84; found C 83.43, H 5.64, N 10.82.

Table S1. Physical data of **DMAC-TRZ** and **PXZ-TRZ**.

	E_{ox} [V]	E_{red} [V]	HOMO [eV]	LUMO [eV]	E_g [eV]
DMAC-TRZ	0.98	-1.47	-5.30	-2.78	2.52
PXZ-TRZ	0.80	-1.49	-5.14	-2.80	2.34

Table S2. The analyzed data based on PL decay cruves of **PXZ-TRZ**- and **DMAC-TRZ** doped films

Molecule	T1	T2	B1	B2	T1*B1	T2*B2	Total	Prompt ratio	delay ratio	Prompt PLQY	delay PLQY
PXZ-TRZ	1.91E-08	1.01E-06	1.24	9.42E-03	2.38E-8	9.53E-9	3.34E-8	0.72	0.29	47.2	18.8
DMAC-TRZ	2.03E-08	1.89E-06	1.32E+00	0.00734	2.67E-08	1.38E-08	4.05E-08	0.66	0.34	55.0	34.5

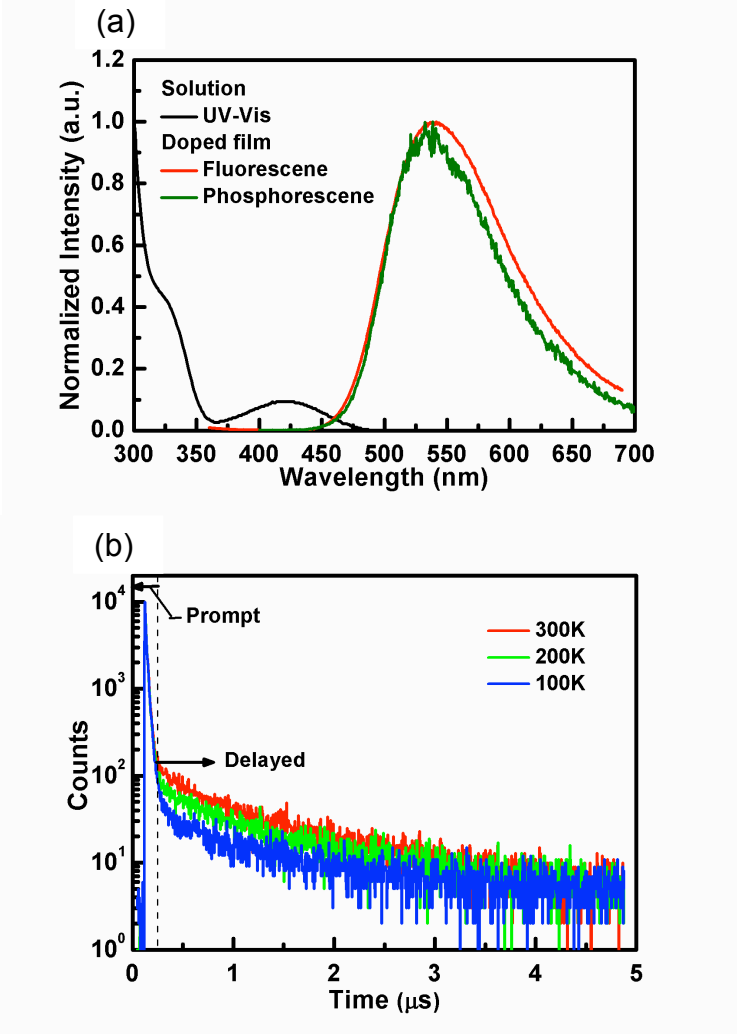

Figure S1. (a) UV-Vis absorption spectrum of **PXZ-TRZ** in solution (toluene), fluorescence spectrum (measured at room temperature) and phosphorescence spectrum (measured at 77 K) of **PXZ-TRZ** doped in mCPCN films (with a doping concentration of 8 wt.%). (b) PL decay cruves of **PXZ-TRZ**-doped films measured at various temperatures.

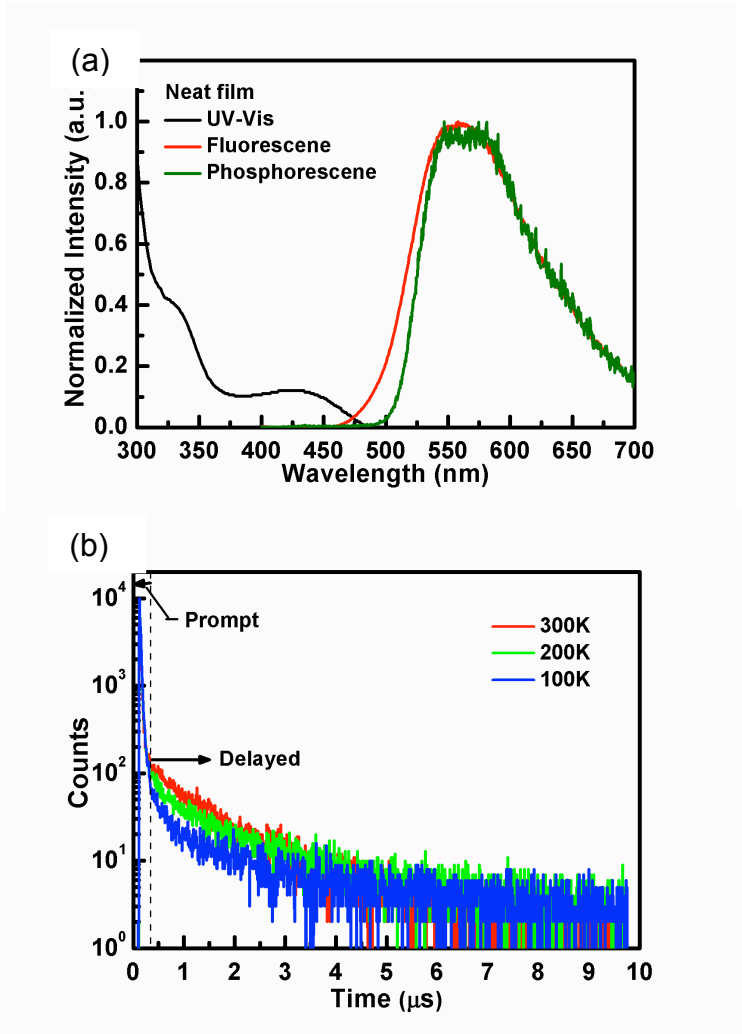

Figure S2. (a) UV-Vis absorption, fluorescence (measured at room temperature), and phosphorescence (measured at 77 K) spectra of **PXZ-TRZ** neat films. (b) PL decay cruves of **PXZ-TRZ** neat films measured at various temperatures.

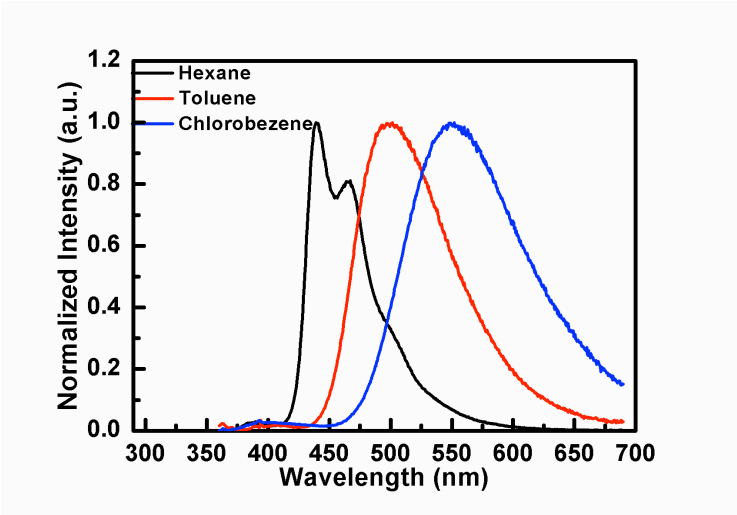

Figure S3. Fluorescence spectra of **DMAC-TRZ** in different solvents.

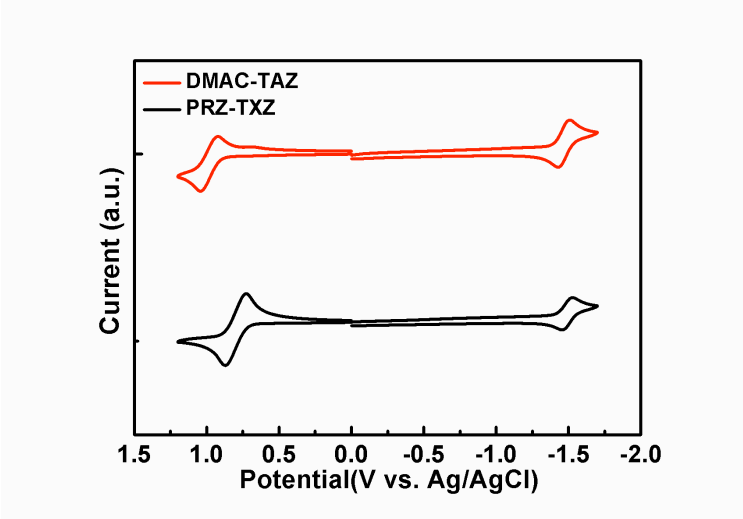

Figure S4. Cyclic voltammogram of **DMAC-TRZ** and **PXZ-TRZ**. The measurement of oxidation potentials was performed in CH_2Cl_2 with 0.1 M of nBu$_4$NPF$_6$ as supporting electrolyte, and the reduction CV was performed in DMF with 0.1 M of nBu$_4$NClO$_4$ as supporting electrolyte.

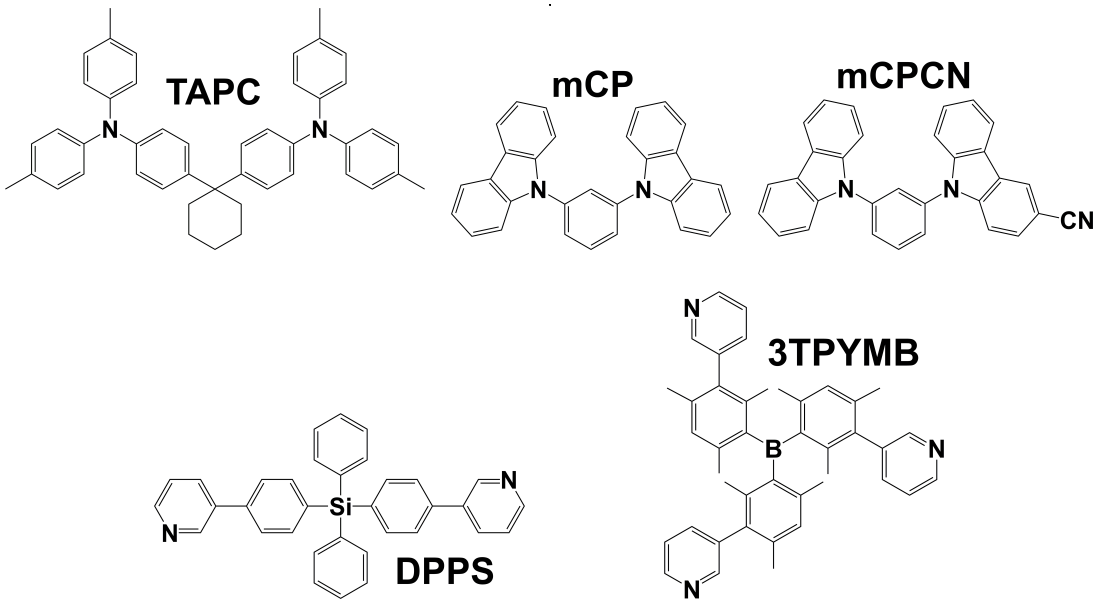

Figure S5. Molecular structures of materials used in OLED devices.

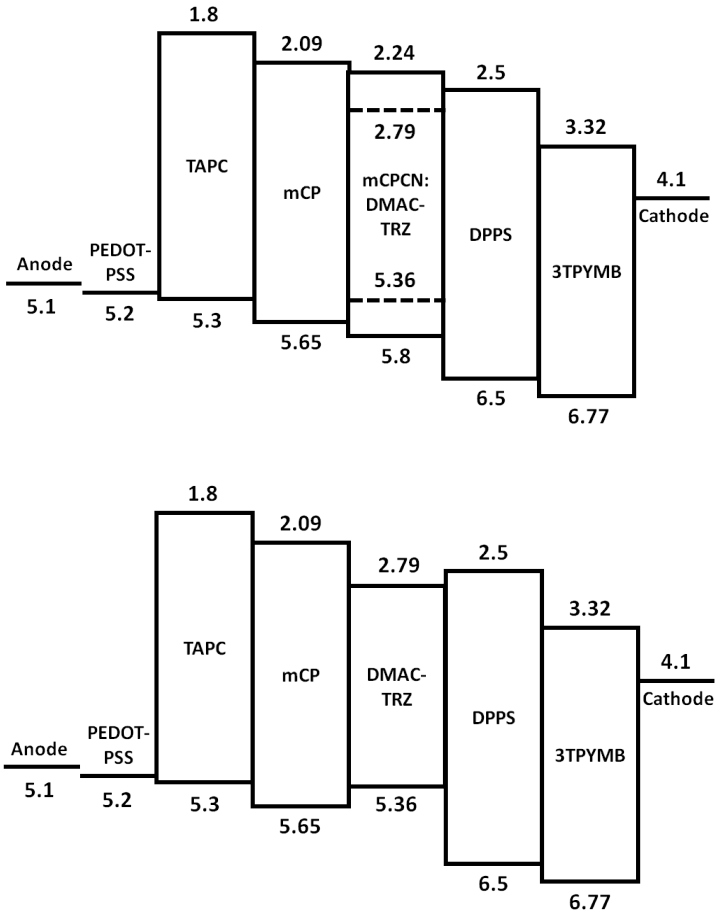

Figure S6. Energy-level diagrams for the doped device (top) and the non-doped device (bottom).

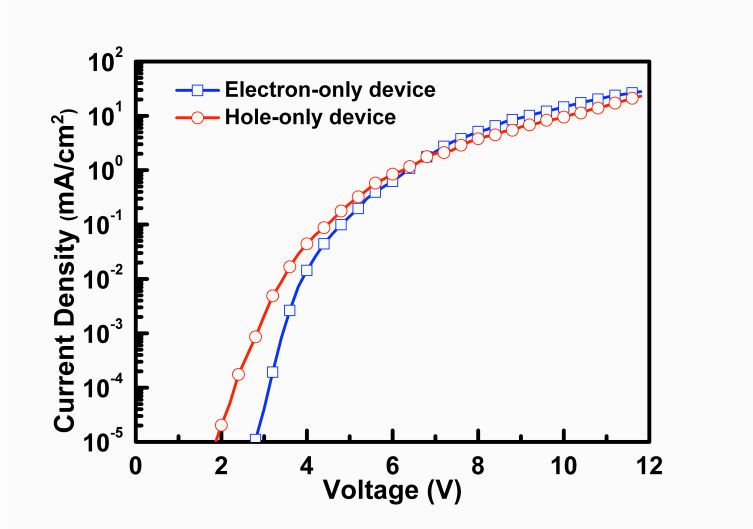

Figure S7. I-V characteristics of the hole-only and electron-only devices. The hole-only device had the structure of: ITO/TAPC (20nm)/mCP (10nm)/DMAC-TRZ (20nm)/TAPC (30nm)/Al (100 nm). The electron-only device had the structure of: ITO/3TPYMB (30nm)/DMAC-TRZ (20nm)/DPPS (5nm)/3TPYMB (30nm)/LiF (1nm)/Al (100 nm).